# Radiative Pion Capture from the 1s Level in $^6$Li

D. Renker, W. Dahme, W. Hering, H. Panke, and Č. Zupančič
*Sektion Physik, Universität München, D-8046 Garching, Germany*

and

J. C. Alder, B. Gabioud, C. Joseph, J. F. Loude, N. Morel, J. P. Perroud, A. Perrenoud, M. T. Tran, and E. Winkelmann
*Institut de Physique Nucléaire, Université de Lausanne, CH-1015 Lausanne, France*

and

G. Strassner and P. Truöl
*Physik-Institut der Universität Zürich, CH-8001 Zürich, Switzerland*

(Received 23 August 1978)

Partial rates for radiative capture from the 1s atomic level in $^6$Li to the lowest two $^6$He states have been determined by measuring, with the necessary energy resolution, x rays and high-energy photons in coincidence. A comparison of our results and other related experimental results with different theoretical approaches shows that phenomenological wave functions consistently describe photopion processes as well as electromagnetic and weak transitions between low-lying $^6$Li and $^6$He states.

Absorption of stopped negative pions in nuclei with the emission of a high-energy photon (radiative capture) is in some sense the simplest pionic nuclear reaction. The wave functions of stopped pions inside light nuclei are rather well known[1] and the radiative capture is adequately described by a simple one-body operator.[2] In particular, the capture from atomic $s$ levels can be treated both in the impulse approximation and by current-algebra techniques and can be related, with a great degree of confidence, to weak and electromagnetic processes involving the same nuclear states or their isobaric analogs.

Previous work on radiative pion capture in nuclei concerned capture from nonseparated atomic levels, but even in a nucleus as light as $^6$Li $s$ levels contribute only about 40% to the total capture rate.[3] In our experiment we isolated radiative capture from the 1s level in $^6$Li by observing the pionic x rays feeding this level in coincidence with high-energy photons. The mass-6 nuclei are a good test case for theoretical predictions in view of the large amount of experimental information on their low-lying states.[4-8]

The experiment was set up in the high-intensity pion beam at the Swiss Institute for Nuclear Research (SIN). A magnetic pair spectrometer[9] detected the high-energy photons. Four shielded 1-mm-thick NaI(Tl) crystals (76 mm in diameter) accepted the low-energy (25 to 30 keV) x rays. The energy resolution of 40% sufficed to separate the transitions to the 1s level from those feeding higher levels, which have energies below 7 keV. For most measurements we used a 100-mm-long cylindrical (diam = 50 mm) target of 94.8% enriched $^6$Li.[10]

A high-energy photon was detected in coincidence with an incoming pion and, whenever a coincident signal from one of the four NaI was observed, the pulse height and the relative timing of the x-ray pulse was recorded. In this way, the high-energy photon spectra, with and without an x ray in coincidence, were measured simultaneously. In order to maximize the acceptance of the pair spectrometer, a 0.052-radiation-length thick photon converter was used. The high-energy photon spectra, both single and coincident, as obtained under these conditions are shown in Fig. 1. The inserts show the upper part of the single spectrum measured with a thinner converter and correspondingly better energy resolution and an x-ray spectrum from one of the NaI crystals.

The relative 1s-absorption rate was extracted from x-ray measurements without the magnetic pair spectrometer in coincidence. The x-ray yield (number of detected x-ray quanta $N_x$ after subtraction of the associated target-out background, divided by the number of stopped pions $N_\pi$) is given by

$$N_x/N_\pi = w_{1s}\,\eta_{\mathrm{NaI}}, \tag{1}$$

where $w_{1s}$ is the probability that the pion populates the 1s level and $\eta_{\mathrm{NaI}}$ is the acceptance of the four NaI crystals including corrections for the absorption of x rays in the target, air, and entrance window. For consistency we compare $w_{1s}$ as determined from Eq. (1) with previous measurements. With $\eta_{\mathrm{NaI}} = (1.75 \pm 0.16) \times 10^{-2}$ we

 

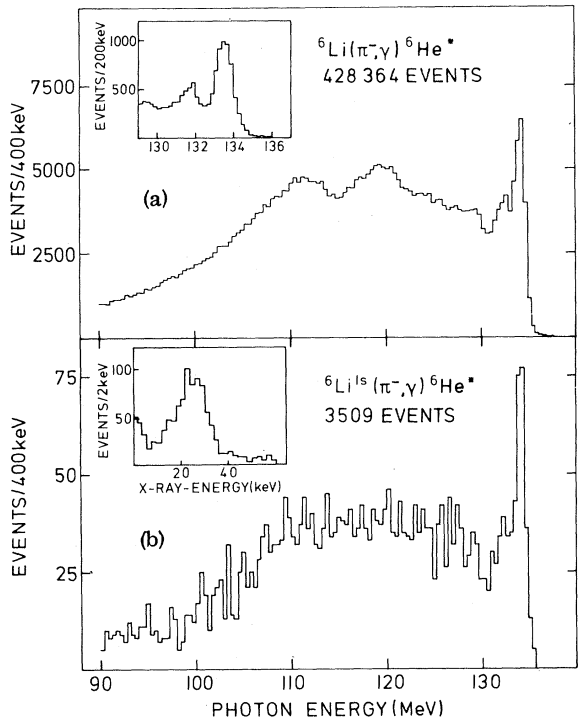


FIG. 1. Spectrum of high-energy photons from radiative pion capture in $^6$Li. (a) Capture from all atomic levels. The inset shows the upper part of the spectrum measured with optimum resolution. (b) Capture from the atomic 1s level. The inset shows the x-ray spectrum from the coincidence measurement.

find $w_{1s}=(35.7\pm5.1)\%$ while Sapp *et al.*[3] find $(33.5\pm6.5)\%$.

The yield of coincidences of high-energy photons with x rays is

$$N_{\gamma x}/N_\pi = w_{1s}(\Lambda_\gamma{}^{1s}/\Lambda_{\rm tot}{}^{1s})\eta_{\rm NaI}\,\eta_{\rm p.s.}, \qquad (2)$$

where $\Lambda_\gamma{}^{1s}$ and $\Lambda_{\rm tot}{}^{1s}$ are the radiative capture and total absorption rate and $\eta_{\rm p.s.}$ is the acceptance of the pair spectrometer, which is known from hydrogen calibration: $\eta_{\rm p.s.}=(4.5\pm0.15)\times10^{-5}$ at 130 MeV.[9] By comparing $N_{\gamma x}/N_\pi$ to $N_x/N_\pi$ we only need to know the acceptance of the pair spectrometer to get the branching ratio $R_{1s}$ for radiative pion capture from the 1s level:

$$R_{1s}=\Lambda_\gamma{}^{1s}/\Lambda_{\rm tot}{}^{1s}=N_{\gamma x}/(N_x\eta_{\rm p.s.}). \qquad (3)$$

The quantities $N_x$ and $N_{\gamma x}$ in Eqs. (1) to (3) are obtained from the raw NaI spectra in the following way. Only NaI pulses within $\pm\frac{1}{2}$ full width at half maximum of the peak are accepted in the analysis. Still there remains a background under the peak which is due mostly to NaI pulses in random coincidence with the incident pion (and the pair spectrometer in case of $N_{\gamma x}$). The spectrum of random pulses was checked to be smooth and the background was determined from a Gaussian-plus-polynomial fit to the total NaI spectrum. This background contributes less than 10% of the events in the peak region and was subtracted under the assumption that it is entirely due to random coincidences. Target impurities contribute no background in the region of the lowest two $^6$He states, to which we restrict the present report.

The $0^+$ ground-state branching ratios are determined by fitting the highest-energy photon line with the known resolution function from the $\pi^-+p\to n+\gamma$ calibration line at 129.4 MeV. However, the $2^+$ first excited state (132.15 MeV) is superimposed on a continuum from the disintegration of $^6$He into $^4{\rm He}+n+n$ (upper-end energy 132.95 MeV), which is further complicated by the $^5{\rm He}_{\rm g.s.}+n$ channel (energy about 132 MeV). Since the position and the width of the $2^+$ state are known ($E_{\rm exc}=1.80$ MeV, $\Gamma=110\pm20$ keV),[11] we fitted our spectrum in this energy region with a Lorentzian line shape of fixed width and position, superimposed on a smooth background which we parametrize by a polynomial in $x=(k_{\gamma\max}-k_\gamma)^{1/2}$, $k_\gamma$ being the photon energy, leaving the cutoff energy $k_{\gamma\max}$ as one of the free parameters. We find the optimum $\chi^2$ with the cutoff energy $k_{\gamma\max}=133$ MeV corresponding to the $^4{\rm He}+n+n$ threshold. The $\chi^2$ does not significantly improve by adding terms beyond second order in $x$.

From the single high-resolution spectrum we obtain the radiative-capture branching ratio $R$ for the sum of $s$ and $p$ contributions. From the coincident spectrum we obtain the 1s branching ratio $R_{1s}$ separately. Under the assumption that radiative branching ratios do not depend on the principal quantum number of the atomic level, the 2p branching ratio $R_{2p}$ may be obtained from the difference between $R$ and $R_{1s}$, and x-ray data.[3] Knowing the widths of the atomic 1s and 2p levels,[3,12] the absolute radiative-capture rates $\Lambda_\gamma{}^{1s}$ and $\Lambda_\gamma{}^{2p}$ may be calculated. The resulting values are $\Lambda_\gamma{}^{1s}=(1.39\pm0.16)\times10^{15}\ {\rm s}^{-1}$, $\Lambda_\gamma{}^{2p}=(5.8\pm1.9)\times10^{10}\ {\rm s}^{-1}$ for the $^6$He ground state and $\Lambda_\gamma{}^{1s}=(0.33\pm0.12)\times10^{15}\ {\rm s}^{-1}$, $\Lambda_\gamma{}^{2p}=(2.5\pm1.1)\times10^{10}\ {\rm s}^{-1}$ for the $^6$He first excited state.

In Table I our results are compared to recent theoretical predictions grouped into two classes, the first of which uses the impulse approximation (IA) while the second is based on the so-called elementary-particle (EP) treatment. In IA calculations the amplitude for radiative capture from

TABLE I. Comparison of our experimental results and recent theoretical predictions for the $^6$He ground state and first excited state. Here, $b$ is the harmonic-oscillator parameter. $R_{1s}$, $R_{2p}$, and $R$ are the radiative-capture branching ratios from the atomic 1$s$ level, the 2$p$ level, and all levels, respectively. $\Lambda_\gamma^{1s}$ and $\Lambda_\gamma^{2p}$ are the absolute radiative-capture rates from the 1$s$ and 2$p$ levels, respectively. The theoretical values obtained in structure-type and phenomenological impulse-approximation calculations are indicated by St and Ph, Respectively. In the latter group, the calculation of Ref. 20 uses $\pi$-capture matrix elements directly obtained from other reactions.

| Wave Function Components | | | | | b | $\Lambda_\gamma^{1s}$ | $\Lambda_\gamma^{2p}$ | Reference | Type |
|---|---|---|---|---|---|---|---|---|---|
| $^6$He(0$^+$) | | $^6$Li(1$^+$) | | | [fm] | [s$^{-1}$] | | | |
| $^1S_0$ | $^3P_0$ | $^3S_1$ | $^1P_1$ | $^3D_1$ | | $10^{15}$ | $10^{10}$ | | |
| .92 | -.40 | .95 | .30 | .02 | 1.95 | 1.70 | 5.4 | 16 | St |
| .93 | -.36 | .99 | .12 | -.03 | 1.95 | 1.89 | 4.8 | 17 | St |
| .92 | -.40 | .95 | .30 | .02 | 1.66 | 2.56 | 3.0 | 18 | St |
| .84 | -.54 | .92 | .37 | .10 | 2.19 | 1.32 | | 5 | Ph |
| 1.00 | -.01 | .92 | .37 | .10 | 2.30 | 1.45 | | 5 | Ph |
| 1.00 | .03 | .92 | .37 | .10 | 2.03 | 1.60 | | 13 | Ph |
| 1.00 | .03 | .92 | .37 | .10 | - | 1.45 | | 13 | Ph |
| - | - | - | - | - | 2.05 | 1.51 | 5.3 | 20 | Ph |
| .89 | .45 | .97 | .25 | .05 | 1.98 | 1.10 | 4.1 | 21 | Ph |
| | | | | | | 1.60 | | | EP |
| Experiment: | | R = .34±.03 % | | | | | | | |
| | | $R_{1s}$ = .47±.05 % | | | | 1.39 ±.16 | 5.8 ±1.9 | this work | |
| | | $R_{2p}$ = .26±.05 % | | | | | | | |
| $^6$He(2$^+$) | | $^6$Li(1$^+$) | | | | | | | |
| $^1D_2$ | $^3P_2$ | $^3S_1$ | $^1P_1$ | $^3D_1$ | | | | | |
| .83 | .53 | .99 | .12 | -.03 | 1.95 | .61 | 3.5 | 17 | St |
| Experiment: | | R = .11±.01 % | | | | | | | |
| | | $R_{1s}$ = .11±.04 % | | | | .33 ±.12 | 2.5 ±1.1 | this work | |
| | | $R_{2p}$ = .11±.04 % | | | | | | | |

the 1$s$ level is proportional to the elementary electric dipole amplitude $E_{0^+}^{\pi^-}$ and to the nuclear matrix element of the spin-density operator[13]; in the EP treatment[14,15] it is proportional to the nuclear axial form factor $F_A(k_\gamma)$. In both cases, the capture rate is suppressed by a distortion factor $R_s^-$ because of the influence of finite nuclear size and strong interactions on the $\pi^-$ wave function. The theoretical values listed in Table I have been adjusted to a common value of the dipole amplitude $|E_{0^+}^{\pi^-}| = (3.26 \pm 0.06) \times 10^{-2} m_\pi^{-1}$ (Ref. 2) and of the distortion factor $R_s^- = 0.654$ (Ref. 14).

The IA calculations depend on the choice of nuclear wave functions for which there are two alternatives. In the structure-type calculations,[16-18] wave functions which describe well the low-lying nuclear level scheme of $^6$Li are used. In the phenomenological approach,[13,19-21] the wave functions are determined without regard to nuclear-level positions from a fit to all known electromagnetic- and weak-interaction properties (excluding pion-capture probabilities and photoproduction cross sections) of a small number of low-lying states and their isobaric analogs. Our results agree best with the predictions of the phenomenological approach.

The EP prediction is unique if one assumes that the axial form factor $F_A(k_\gamma)$ varies as the magnetic form factor $F_M(q)$, measured in inelastic electron scattering, and takes $F_A(0)$ from $^6$He $\beta$ decay. Using the latest experimental data[5,13] on $F_M(q)$ and the correction to the soft-pion limit from Ref. 15, one arrives at a prediction for $\Lambda_\gamma^{1s}$ to $^6$He$_{g.s.}$ which is 1.2 standard deviation larger than the experimental value. Since the IA calculations[5,13] of the axial matrix element indicate a 3–5% smaller value for $F_A(k_\gamma)$ than that obtained from the above prescription, our results confirm the theoretical estimates[22] that the renormalization of the axial coupling in $^6$Li is small.

Our $\Lambda_\gamma^{1s}$ to $^6$He$_{g.s.}$ is in very good agreement with measurements of the reaction $^6$Li($\gamma$, $\pi^+$)$^6$He$_{g.s.}$ near threshold.[7,13] Apart from kinematical factors, the two processes differ in the center-of-mass photon energies $k_\gamma^- = 134$ MeV and $k_\gamma^+ = 142$ MeV, and in the pion-wave-function distortion factors $R_s^-$ and $R_s^+$. If one accepts the values obtained from the Krell-Ericson potential, i.e., $R_s^- = 0.654$ (Ref. 14) and $R_s^+ = 0.957$ (Ref. 5) ($R_s^-/R_s^+ = 0.683$), the combined results of the two experiments yield $F_A(k_\gamma^-)/F_A(k_\gamma^+) = 1.14 \pm 0.07$ as compared to $F_M(k_\gamma^-)/F_M(k_\gamma^+) = 1.12$ (Refs. 5 and 13).

The only theoretical prediction[17] for the $^6$He (2$^+$, 1.8 MeV) transition exceeds the experimental value for $\Lambda_\gamma^{1s}$ by a factor of 2. However, the ratio $\alpha^{1s} = \Lambda_\gamma^{1s}(2^+)/\Lambda_\gamma^{1s}(0^+)$ is theroetically predicted to be $\alpha^{1s} = 0.32$, in fair agreement with the experimental value $\alpha^{1s} = 0.24 \pm 0.09$. The difference between our result for $\alpha^{1s}$ and the equivalent one from threshold photopion production $\alpha^{1s} = 0.80 \pm 0.30$ can be traced to the disregard of the important $^4$He + $n$ + $n$ continuum in the analysis of

the photopion experiment. The ratio of the squares of electromagnetic transition form factors to the $2^+$ and $0^+$ states in $^6$Li at the momentum transfer corresponding to radiative pion capture is 0.22 ±0.08 (Refs. 5 and 6), again confirming the close relation between the axial and magnetic form factors.

We gratefully acknowledge the support of SIN under the directorate of Professor J. P. Blaser. This research was also supported by the German Federal Ministry for Research and Technology (BMFT) and the Swiss National Science Foundation.

[1]J. Hüfner, Phys. Rep. 21C, 1 (1975).
[2]For a review of previous experimental and theoretical work, see H. W. Baer, K. M. Crowe, and P. Truöl, Advan. Nucl. Phys. 9, 177 (1977).
[3]W. W. Sapp *et al.*, Phys. Rev. C 5, 690 (1972).
[4]J. P. Deutsch *et al.*, Phys. Lett. 26B, 315 (1968).
[5]J. C. Bergström, I. P. Auer, and R. S. Hicks, Nucl. Phys. A251, 401 (1975).
[6]R. Neuhausen and R. M. Hutcheon, Nucl. Phys. A164, 497 (1971).
[7]G. Audit *et al.*, Phys. Rev. C 15, 1415 (1977).
[8]F. Ajzenberg-Selove and T. Lauritsen, Nucl. Phys. A227, 1 (1974).
[9]J. C. Alder *et al.*, to be published.
[10]We thank K. Crowe and J. A. Bistirlich (Berkeley) and C. Tzara and N. de Botton (Saclay) for the generous loan of their targets.
[11]F. Ajzenberg-Selove, J. W. Watson, and R. Middleton, Phys. Rev. 139, B592 (1965).
[12]G. Backenstoss *et al.*, Nucl. Phys. B66, 125 (1973).
[13]J. B. Cammarata and T. W. Donelly, Nucl. Phys. A267, 365 (1976).
[14]J. Delorme, Nucl. Phys. B19, 573 (1970).
[15]M. Ericson and M. Rho, Phys. Rep. 5C, 58 (1975).
[16]J. D. Vergados, Nucl. Phys. A220, 259 (1974).
[17]G. E. Dogotar *et al.*, Nucl. Phys. A282, 474 (1977); Dubna Report No. JINR E2-10509, 1977 (unpublished).
[18]J. D. Vergados and H. W. Baer, Phys. Lett. 41B, 560 (1972).
[19]J. C. Bergström, personal communication to H. W. Baer.
[20]W. Maguire and C. Werntz, Nucl. Phys. A205, 211 (1973).
[21]F. Roig and P. Pascual, Nucl. Phys. B66, 173 (1973).
[22]J. Delorme, M. Ericson, and G. Fäldt, Nucl. Phys. A240, 493 (1975).

# Rotational Bands in Asymmetrically Deformed $^{231}$Th

J. Blons, C. Mazur, D. Paya, and M. Ribrag
*Département de Physique Nucléaire, Centre d'Etudes Nucléaires de Saclay, 91190 Gif-sur-Yvette, France*

and

H. Weigmann
*Central Bureau for Nuclear Measurements, EURATOM, Geel, Belgium*

(Received 7 August 1978)

The neutron-induced fission cross section of $^{230}$Th near 720 keV is resolved into sharp structures interpreted as two rotational bands with opposite parities, indicating an asymmetrically deformed third minimum in the fission barrier.

The $^{230}$Th$(n,f)$ cross section has long been known to exhibit a well-isolated peak at 720 keV neutron energy with a full width at half maximum (FWHM) of 35 keV. It was interpreted as a pure vibrational state in the secondary minimum of the Strutinsky potential-energy curve. From angular distribution considerations, an intrinsic state with $K=\frac{1}{2}$ was associated with this vibration and assumed to be the head of a rotational band. Equally good fits to the data were obtained for $K=\frac{1}{2}^+$ and $K=\frac{1}{2}^-$.[1,2] In addition, since no individual level was observed across the peak, it was difficult to deduce the moment of inertia and the decoupling parameter.

On the other hand, our measurements of the $^{232}$Th$(n,f)$ cross section showed a fine structure in the peak at 1.6 MeV neutron energy, which we interpreted as a rotational band in a shallow third minimum of the potential energy curve.[3] From intensity considerations it was necessary to assume that both positive and negative parities were present.[4] In fact, the presence of two close-lying rotational bands with opposite parities can be understood as being a consequence of the asymmetric deformation expected for the third minimum[5,6]: The wave functions of stationary states

 